Observations on the Transition Process of Two-Dimensional Supersonic Wakes

ANTHONY DEMETRIADES*
Philco-Ford Corporation, Newport Beach, Calif.

A detailed study has been made of the flow properties in the two-dimensional supersonic wake behind a heated slender flat plate. This wake exhibits a sequence of well-defined laminar, transitional, and turbulent regimes. The data included the mean (average) properties, the modally-resolved fluctuations and their spectra, and the fluctuation scales. The lateral wake profiles first depart from laminar similarity at the virtual origin of turbulence and reach turbulent similarity 500 thicknesses later; a large increase in kinematic viscosity and a small decrease in Prandtl number mark the transition zone. The wide-band fluctuations increase smoothly and the scales decrease greatly through transition towards magnitudes representative of turbulent wakes. However fluctuations as high as 10% of the deficits, as well as distinct scale sizes, were noted in the pretransitional wake. Spectrum analysis suggested that this is because of a laminar oscillation fitting in the predictions of laminar stability theory. Evidence was gathered that this oscillation triggers transition by spectral dispersion and remains visible in the turbulent wake, perhaps as a turbulence instability.

I. Introduction

IT has been known for some time that wakes generated by bodies moving at high speeds can exhibit a complete laminar-transitional-turbulent sequence, with the transition distance often removed from the body by a considerable distance. In the early 1960's a number of experiments were performed to detect this distance for a variety of body shapes and flight speeds, and especially to find its dependence on the flight Reynolds number. Although transition-distance correlations[1] have served a practical purpose, they have located the region of transition only approximately and they have done nothing to describe quantitatively the phenomena within it.

One general problem area regarding wake transition lies on its mechanism. It is often the case that turbulence onset follows the amplification of periodic disturbances, and the instability modes, wavelengths and amplification rates have been studied theoretically in the linear[2] and nonlinear[3,4] regimes for cases including compressibility and heat transfer. Periodicity in the laminar wake structure is sometimes observed in wakes of hypervelocity projectiles[5,6] but its connection to profile instability is often obscure. However, Behrens[7] has reported instabilities in inviscid hypersonic wakes while Batt[8] and this author[9] have demonstrated, using cooled and heated bodies, that the transition zone in a high-speed wake is accelerated or delayed, respectively, in agreement with theoretical predictions on the effect of heat transfer on small disturbance growth. Just recently Behrens and Ko[10] detected instabilities in the inner laminar hypersonic wake of a slender body, whose wavelengths and growth rates matched the expectations of small disturbance theory.

A closely related area of interest concerns the extent of the transition zone and its appended turbulent relaxation length, and the evolution of the mean flow properties and fluctuation magnitudes from the equilibrium laminar to the equilibrium turbulent states. The virtual origin of turbulence and the initial conditions of the turbulent wake are important to know in engineering applications and, if long enough, the transition-relaxation zone is important to understand on its own merits because it cannot be described by similarity rules. As always, data are scarce because of the experimental hardships of measuring turbulence in compressible flows. For example, Favre[11] who made the first definitive study of microscopic structure in the transition zone, did not resolve this structure into velocity and density contributions.

The purpose of the present experiment was to make fully resolved measurements in a wake transition zone in order to detect the gradual change of flow properties along its length and, to a lesser extent, to assess the role of chance instabilities in the transition process. The transitional wake chosen was preceded by a clearly-defined laminar wake and followed by an equally well-defined turbulent wake. The starting conditions and final limits of flow properties in this zone were thus known to conform with expectations from theory or previous experiments. By employing a very slender high-aspect-ratio body adequate two-dimensionality was achieved and all inviscid gradients were removed.

II. Experiment Design

A two-dimensional wake at Mach number 3.0 and Reynolds number 70,000/cm was produced by stretching a thin steel ribbon at zero incidence across the test-section of the Philco-Ford Supersonic Wind Tunnel operated at a total pressure P_0 = 730 mm Hg absolute and total temperature T_0 = 38°C. In this respect, the experiment was identical to the study of the fully-turbulent adiabatic wake behind this ribbon whose mean and turbulence properties were reported in detail in Refs. 12 and 13. The slenderness of the ribbon (chord of 0.294 cm and thickness of 0.01 cm) minimized the leading-edge and wake shock effects to the point where the edge conditions of the wake were very nearly equal to the freestream values.

Under the tunnel conditions mentioned previously natural transition occurs very near the trailing edge of the model.[12] To minimize the proximity effects of the model, it was necessary to remove the transition zone as far downstream as

Presented as Paper 70-793 at the AIAA 3rd Fluid and Plasma Dynamics Conference, Los Angeles, Calif., June 29–July 1, 1970; submitted November 12, 1970; revision received April 23, 1971. This work was sponsored by the Advanced Research Projects Agency and monitored by the U. S. Air Force under Contract FO4701-69-C-0118.

Index categories: Supersonic and Hypersonic Flow; Boundary-Layer Stability and Transition; Jets and Wakes, and Viscid-Inviscid Flow Interactions.

* Supervisor, Experimental Aerodynamics Section. Associate Fellow AIAA.

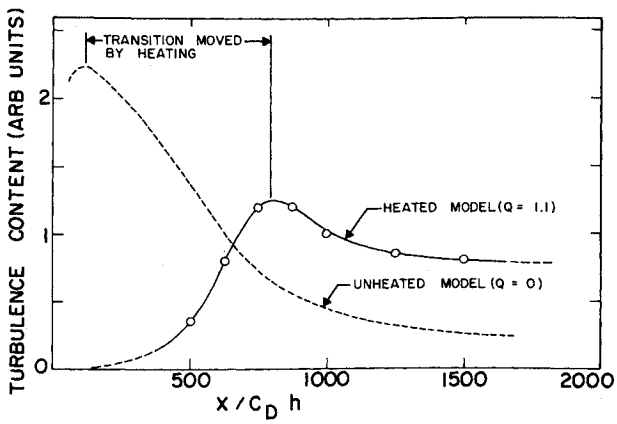

Fig. 1 Variation of raw hot-wire rms voltage output along the wake centerplane; signal maximum is often defined as the transition point.

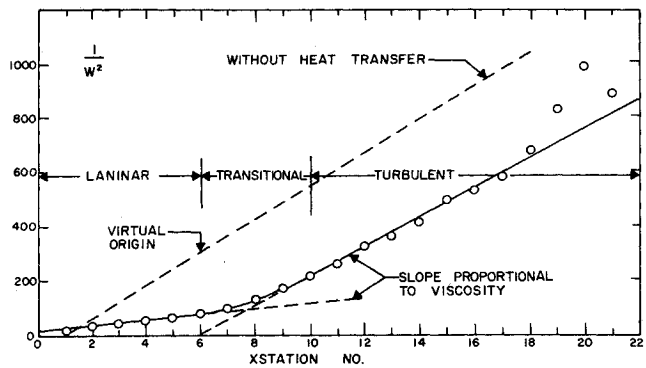

Fig. 2 Variation of measured inverse-squared velocity defect along centerline of wake.

feasible. Delaying transition by lowering P_0 was possible but undesirable, since this would decrease the Reynolds number and upset the precarious dynamic equilibration of the turbulence.[12] Transition delay was finally achieved by heating the model electrically with a well-regulated d.c. power supply to the highest practical temperature. As already noted in the introduction, body heating stabilizes the wake and it was indeed found that transition was moved considerably downstream. The heating power was 87 w which corresponds to a ratio $Q \equiv$ power transferred to the flow/kinetic power of wake = 1.1 where the kinetic wake power is defined as $\frac{1}{2}\rho_\infty u_\infty^3 C_D h$. Reference 9 gives details on the effect of Q on the transition distance location. The exact transition location for $Q = 1.1$ will be discussed below.

The measuring instruments are described at some length in Refs. 12 and 13. Mean-flow data were verified by redundant measurements. Turbulence measurements were made with a 0.00005-in.-diam constant-current hot wire and were specifically and laboriously designed to resolve the individual modes (velocity u and temperature T) contributing to the signal. This resolution, which was extended to the turbulent spectra as well as the wideband fluctuations, was a major lack in the earlier work dealing with the phenomenology of transition. Measurements were made along a direction Y normal to the plane of the wake at 21 positions X along the midspan line (these are called "XSTATIONS") spaced 0.300 in. apart.

III. Mean Flow in the Transition Zone

The first task in this work was to make a qualitative determination of the location of transition. Frequently this can be done by observing the variation of the unresolved mean-square output of the hot-wire along the flow;[14] a convenient, although not accurate, definition is the maximum of this output, which is supposed to occur after the growth of nonlinear disturbances but still prior to turbulent diffusion. Figure 1 shows that this maximum lies at about 800 drag thicknesses $C_D h$ behind the model, which physically corresponds to a distance of about 10 cm. We shall return to the quantitative interpretation of this signal in Sec. IV.

Figure 2 shows the variation of the (inverse squared) "velocity defect" $w \equiv [u_\infty - u(0)]/u_\infty$ along the centerline, where ∞ refers to conditions outside and (0) to those on the centerline of the wake. Although the $w \sim (X)^{-1/2}$ decrease expected for both laminar and turbulent wakes holds for the entire range of data two distinct regions are apparent. The slope of the curve is proportional to the viscosity[12,15] and it is seen to increase greatly from the upstream to the downstream region. In the latter the slope of the experimental curve agrees well with that of the turbulent wake without heat transfer,[12] for which transition occurred near XSTATION 1 (see dashed lines on Figs. 1 and 2). Furthermore, the data for the latter experiment were in perfect numerical agreement with the well-known behavior of low-speed two-dimensional turbulent wakes as reported by Townsend.[15]

The virtual origin of turbulence X_0 can be considered to lie at XSTATION 6. Using the wake drag thickness $C_D h$ which was measured to be nearly constant along the entire wake length, we define the proper axial coordinate for turbulence growth along the wake as $\bar{X} \equiv (X - X_0)/C_D h$. Note that by this definition the model midchord line lies at $\bar{X} = -532$ and the farthest downstream XSTATION (No. 22) at $\bar{X} = 1216$. The transition zone can, for the present, be identified only as the region where the two different regimes in the data of Fig. 2 are joined smoothly.

Other flow properties showed a variation on the axis as found for the velocity. The velocity defect is replotted, along with the temperature defect $\theta \equiv [T(0) - T_\infty]/T_\infty$ and the wake half-thickness Y^* on Fig. 3. This plot is especially useful in showing the $X^{-1/2}$ slope of the data in the laminar portion of the wake; the choice of coordinate origin obscures this dependence in the turbulent portion beyond $\bar{X} = 500$.

Even more telling as indicators of the transition region are the lateral profiles of velocity and temperature plotted in

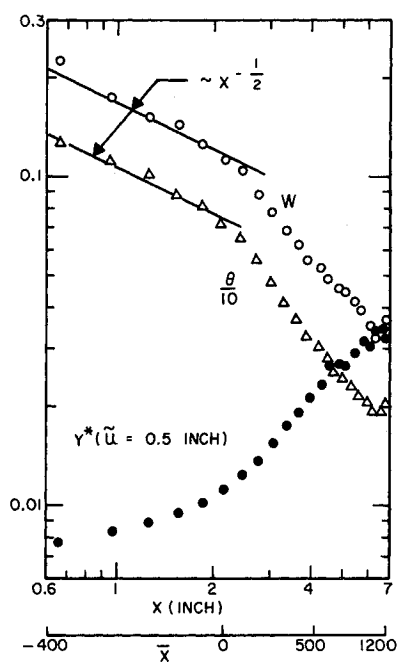

Fig. 3 Variation of velocity and temperature defects and of the wake half-thickness along the centerline.

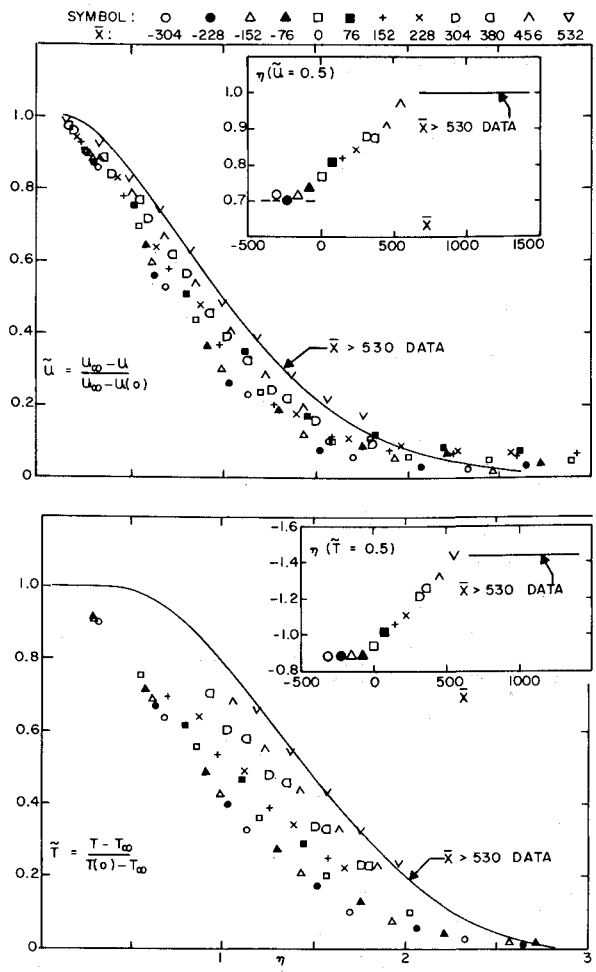

Fig. 4 Lateral profiles of nondimensional velocity and temperature; data in the turbulent wake are shown by solid lines; the nondimensional coordinate η is computed using the measured drag as averaged for the entire wake.

Fig. 4. These plots use the nondimensional coordinates

$$\tilde{u} \equiv \frac{u_\infty - u}{u_\infty - u(0)}, \quad \tilde{T} \equiv \frac{T - T_\infty}{T(0) - T_\infty}, \quad \eta \equiv \frac{\tilde{Y}}{L} \qquad (1)$$

where $\tilde{Y}$ is the Howarth-Dorodnitzyn distance and L the transverse scale $L \equiv (C_D h)/4w$. The flow profiles show strong indications of similarity for negative $\bar{X}$ and a clear departure just prior to $\bar{X} = 0$ toward a larger thickness. The points past $X = 550$ are not plotted since they clustered quite well around the self-similar turbulent profiles shown on Fig. 4 by solid lines. The latter line for the velocity follows $\tilde{u} = e^{-0.69\eta^2}$ which is common to two-dimensional turbulent wakes as found by Townsend at low speeds[15] and lately by this author at Mach 3.0.[12] In the latter reference, the temperature profile shown was also found to agree well with the solid line of Fig. 4.

The differences between the laminar and turbulent profiles of Fig. 4 are here accentuated since in computing L as defined previously, and hence η, the average $C_D h$ was used as obtained for all XSTATIONS along the wake. Although $C_D h$ was indeed nearly constant within the scatter over most of the wake, very near the body it was smaller by a factor of about 20%, possibly because of the drag swallowing.[16] Applying this correction to the first few laminar profiles of $\tilde{u}$ and $\tilde{T}$ has the effect of increasing η and moving all data shown closer together. In fact, the laminar theory of Gold,[17] if adapted to the conditions and nomenclature of this experiment, gives a $\tilde{u}$ profile as shown by the last equation, but with the factor -0.69 changed to -0.785 which is not far removed from the solid line of Fig. 4.

The variation of transport properties along the wake can be found from the measured axis properties shown so far. The variation of the kinematic viscosity ν and Prandtl number σ can be found from the data, for the two-dimensional compressible wake at hand, from formulas which are the same in the laminar[17] and the turbulent flow for σ_T: $\sigma_T = [\theta/w(\gamma - 1)M_\infty^2(1 + Q)]^2$ and nearly the same for the kinematic viscosity: $\nu = u_\infty(C_D h)^2/A^2 X w^2$ with $A = 7.1$ for the laminar and $A = 6.4$ for the turbulent wake. Using the measured values of u_∞, w, M_∞, θ, $C_D h$, and Q, one can plot σ_T and ν vs X for each point on the axis and compare these with their molecular counterparts as done on Fig. 5. The Prandtl number does not vary greatly along the transition zone and reaches $\sigma_T \simeq 0.65$ in the turbulent wake (as also found in Ref. 12 and elsewhere).[18] The kinematic viscsoity is close to the molecular value in the laminar wake but further along it increases and exceeds the laminar level by a factor of nearly 10. A similar increase, although numerically larger because of different conditions, was noted by McCarthy.[19] Finally, the turbulent Reynolds number R_T in the turbulent part of the wake averaged 13.8, close to $R_T = 13.0$ found in Ref. 12 and $R_T = 12.4$ obtained long ago by Townsend.[15]

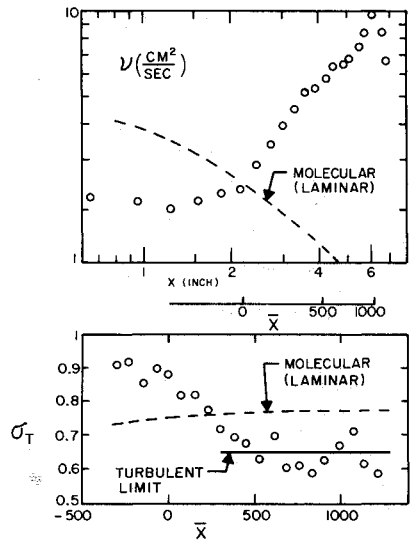

Fig. 5 Variation of the bulk kinematic viscosity and turbulent Prandtl number along the wake centerline.

IV. Fluctuation Intensities

The measurements of mean properties discussed previously bring out the fact that the transition zone is relatively long

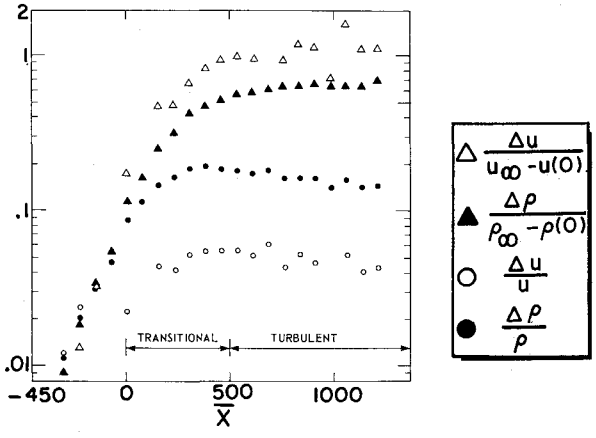

Fig. 6 Wideband rms fluctuations of velocity and density along the wake centerline normalized alternately with the local deficits and local mean values.

and that the virtual origin of turbulence, at $\bar{X} = 0$, coincides closely with the point in the wake where the first departures of the lateral velocity and temperature profiles from laminar similarity are noted. Let us now examine the evolution of the fluctuations themselves along this transition zone.

The growth of wideband, local, rms axial velocity and density fluctuations on the wake centerplane is shown on Fig. 6 normalized alternately with the local mean values and also the deficits $u_\infty - u(0)$ and $\rho_\infty - \rho(0)$, where ∞ and (0) refer to the external and centerplane fluid, respectively. The terms transitional and turbulent here refer, again, to the state of the flow as deduced from the mean measurements. In the turbulent wake, the fluctuations reach a large and constant magnitude,† near $\bar{X} = 500$ where the transition process is nearly complete. At the beginning of the transition zone the rms fluctuations are approximately 10% of their respective deficits; they are much smaller, nearly 1% of the deficits, at a point 300 thickness upstream of the transition zone.

The one-dimensional spectra, which will be discussed farther below, yielded the integral longitudinal scales Λ of velocity and temperature shown on Fig. 7. The scales Λ_u and Λ_T are normalized both with the thickness $C_D h$ and the transverse scale L. Both Λ_u and Λ_T are found here to be about equal to each other and to tend toward $4C_D h$. However, the representation Λ/L allows a much better indication of scale change since L is proportional to the physical (and changing as $X^{1/2}$) wake thickness. Considering that L is nearly equal to the wake half thickness [see Eq. (1) and Fig. 4], we can say that these scales begin from a size many times this half thickness in the laminar wake and end up nearly equal to $L/2$ in the turbulence. Such a drastic reduction of these important physical subdivisions of the fluid imply a fractionization of its structure such as turbulence alone can create. Favre[11] has observed a similar decrease of the turbulence microscale in the transition zone of a supersonic wake configured much like the one studied here.

Still, Figs. 6 and 7 imply a certain amount of turbulence activity in the laminar wake as well, and especially a phenomenon having a large but distinct scale length and a fluctuation intensity ranging up to 10% of the mean wake deficits. This phenomenon was clarified with the aid of the spectrum measurements described below.

V. Spectra of the Fluctuations

The Eulerian (single-point) spectra of the wake fluctuations were measured at alternating XSTATIONS along the wake ($\bar{X} = -228, -76, 76, 228, \ldots$) and at several lateral positions at each $\bar{X}$. The contribution of the vorticity (velocity) and entropy (temperature) modes to each spectrum was resolved by the usual assumption of negligible sound intensity and by subjecting the raw data to a modal analysis within each passband.[20] The viscous cutoff frequency was estimated at about 2.5 MHz, and signals as high as 1.5 MHz were in fact detected. The characteristic wake frequency, based on a flow speed of about 60,000 cm/sec and a physical wake thickness of order $\frac{1}{8}$ cm, was of order 200 kHz.

Thus resolved, spectra of the velocity and temperature fluctuations, represented by τ and σ, respectively, are shown on Figs. 8 and 9. The nondimensional ordinate of the spectra is the mean-square fluctuation density at frequency f divided by its counterpart at $f = 0$. All data shown here were taken at or near the maximum shear region ($\eta \simeq 1$).

A distinctive spectral peak in the vicinity of 200–400 kHz characterizes each curve. At the beginning, the peak is a subsidiary feature of the spectrum, dominates it in the transition

† The numerical limit of the velocity fluctuations in the turbulent wake, as shown on Fig. 6, is higher than would be expected from previous experience.[13,15] It is not obvious that heat transfer alone can account for this difference, but a discussion of this point is beyond the present purposes.

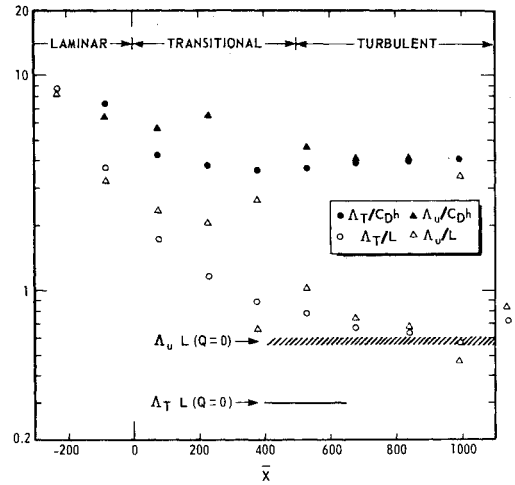

Fig. 7 Longitudinal integral scales of velocity and temperature fluctuations normalized alternately with the local transverse scale L and the average drag $C_D h$.

zone and gradually vanishes in the turbulent wake. Spectral peaks of this type have regularly been found in wake flows studied in this laboratory for some years, with no evidence associating them to extraneous sources.[20] For example, the fundamental vibration frequency of the model is about 100 times smaller than the peak frequency. Furthermore, the logarithmic plot of Figs. 8 and 9 obscures the fact that the peak is actually quite diffuse, whereas mechanical oscillations (including strain-gage vibrations of the hot wire) are invariably very sharp and unrepeatable.

The existence of this prominence in the spectra explains tentatively why a nonvanishing fluctuation intensity and a distinct scale length were observed in the laminar wake (Figs. 6 and 7). The question now becomes one of the source of this fluctuation. In a similar experiment with an axisymmetric wake,[20,21] this author found that the spectral peak (occurring at an altogether different frequency) was characteristic of the turbulent wake rather than of the transition process. This fluctuation had a wavelength of order $10L$ and was identified as a periodic corrugation of the turbulent front.[21] Periodicities of turbulent fronts (interfaces) are apparently possible on theoretical grounds[22] and have been observed for some time in various turbulent flows.[23] Subsequently a similar peak was found in a two-dimensional supersonic turbulent wake,[13] with a wavelength now closer to $3L$—a difference mainly attributable to the difference in geometry. Since this peak persisted in the turbulence for a length of order 1000 wake thicknesses, it was judged unlikely that it could be due to laminar instability remnants.‡ It was not clear, in that experiment, whether that fluctuation was connected to the laminar wake. On the other hand, it did appear in the transitional portion of that wake, very close behind the plate.

Figures 8 and 9 show that the spectral peak observed in the present experiment exists in all three regimes; laminar, transitional and turbulent. It cannot therefore be a purely turbulent phenomenon, whereas if it is due to laminar instability, its long persistence in the turbulent wake is hard to explain.

In support of the laminar-instability argument, Fig. 10 plots the laminar oscillation frequency observed behind slender two-dimensional plates at low speeds by Sato and Kuriki.[24] These authors have suggested that, on the basis of their data, the frequency of laminar oscillations increases as the $\frac{3}{2}$-power of flow speed, which predicts very accurately the frequency observed in the present experiment; modern stabil-

‡ The equivalence between the effective wake thickness $C_D h$ of Ref. 12 and the low-speed flow cylinder diameter[15] was demonstrated on p. 30 of the Reference.

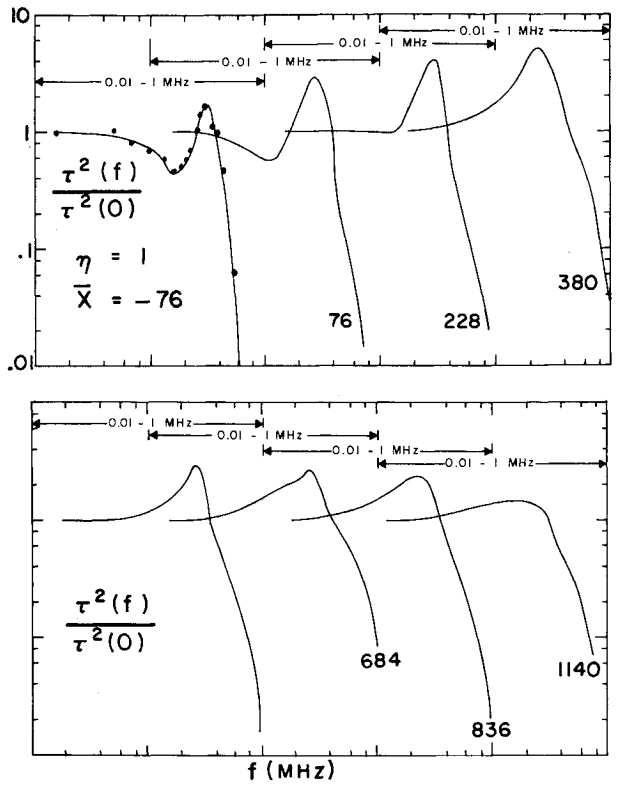

Fig. 8 One-dimensional (longitudinal) spectra of the velocity fluctuations for various axial positions along the maximum shear region of the wake.

ity theory also supports Sato's prediction. Furthermore, the growth and eventual decay of this oscillation is illustrated in Fig. 11 in three alternate ways. In one of the mean-square spectral density (the fluctuation intensity in a sharply-filtered 9.6-kHz band around the peak frequency) of the density-temperature fluctuations normalized with the mean local density fluctuations is followed along the maximum-shear region. This shows the variation of the absolute peak fluctuation magnitude and thus conforms best with similar measures of intensity variation, for example as shown on Fig. 6.

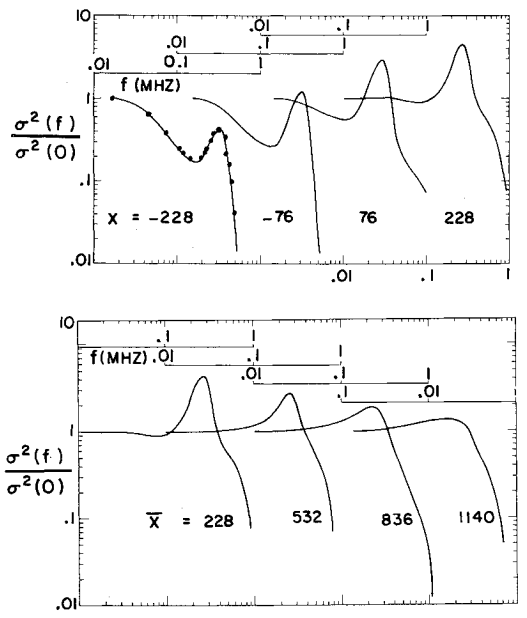

Fig. 9 One-dimensional (longitudinal) spectra of the density fluctuations for various axial positions along the maximum shear region of the wake.

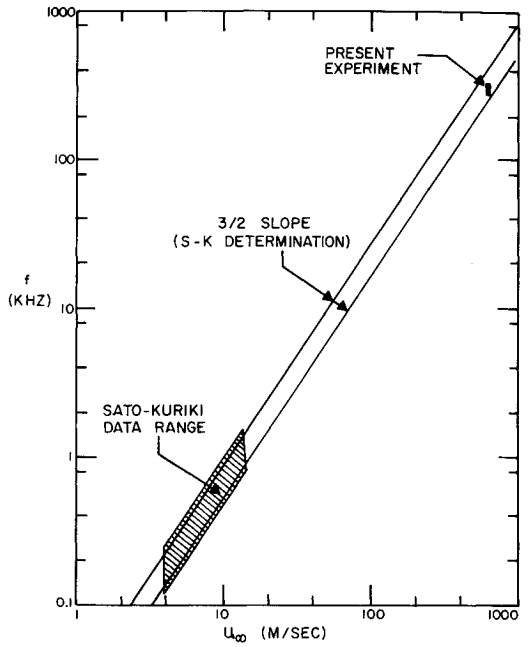

Fig. 10 Dependence of oscillation frequencies in the laminar wake of thin flat plates as a function of flow speed.

Figure 11b shows the intensity of the peak magnitude relative to all the rest of the Fourier components at each point in the wake. We see that the observed oscillation contributes substantially to the total signal in the laminar wake ($\bar{X} < 0$) and that this contribution becomes greatest at the onset of transition ($\bar{X} = 0$); thereafter the importance of the peak decreases relative to the over-all turbulence intensity. Similarly, the peak intensity relative to the spectrum density $\sigma^2(0)$ at zero frequency is shown in Fig. 11c. This is a measure of the flatness of the spectrum at the low-frequency limit, and we see that in the far wake the ratio $\sigma^2(f)/\sigma^2(0)$

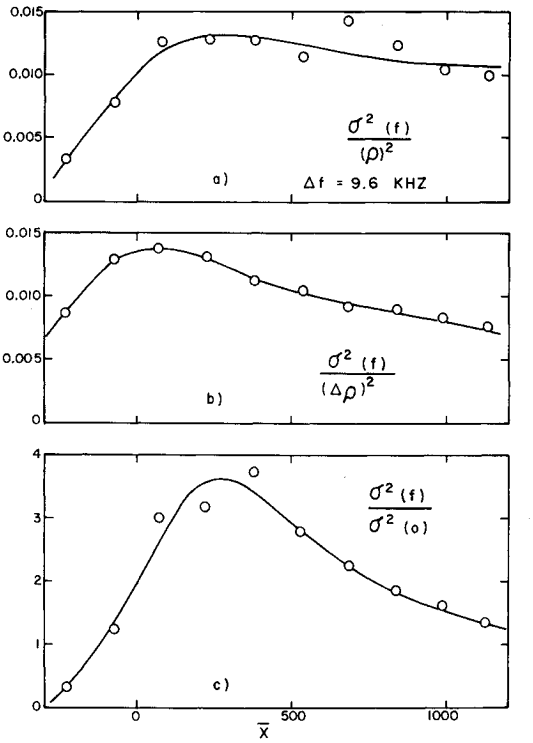

Fig. 11 Variation of spectral density of the density/temperature fluctuations in the vicinity of the observed spectral peak; data are from spectra near maximum shear and are shown normalized in alternate ways.

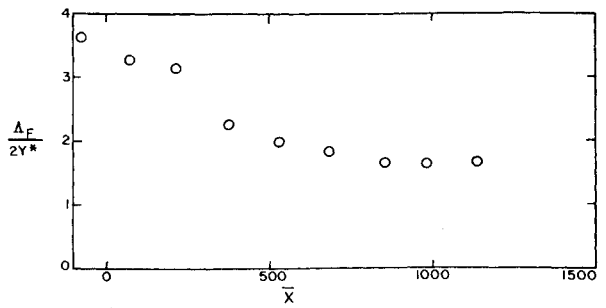

Fig. 12 Axial variation, along the maximum-shear region, of the wavelength of the spectral peak.

approaches unity, meaning that the spectral density is nearly constant below 200 kHz. These density data, which are taken again near the maximum-shear region ($0.9 < \eta < 1.15$) are very closely duplicated by the velocity spectra as well.

A careful examination of Fig. 9 reveals that the peak frequency decreases along the wake. Actually this frequency is near 400 kHz in the laminar wake and decreases to just below 200 kHz in the turbulent wake. The corresponding wavelength Λ_F computed with the local mean velocity therefore increases, but so does the wake thickness. If Λ_F is normalized with the thickness defined by $2Y^* \equiv 2Y(\tilde{u} = 0.5)$, then Fig. 12 shows that the wavelength in fact decreases between the laminar ($\Lambda_F \simeq 4 \times 2Y^*$) and turbulent ($\Lambda_F \simeq 1.7 \times 2Y^*$) wakes by more than a factor of 2. Furthermore, since $Y^* \simeq L$ in the far turbulent wake almost exactly (see Fig. 4), we obtain $\Lambda_F \simeq 3.4L$ which agrees with the data of Ref. 13.

The possibility that the oscillation as observed in the laminar region is due to laminar instabilities is also supported strongly by recent calculations by Behrens.[10] According to his results compressibility does not greatly change the most unstable wavelength in a two-dimensional wake. In our nomenclature, this wavelength is $\Lambda/Y^* = 2\pi/0.8 = 7.8$ which compares most favorably with the value $\Lambda_F = 8Y^*$ found from Fig. 12.

However, in the turbulent wake ($\bar{X} > 500$) where $\Lambda_F/2Y^*$ goes below 2, the nature of the oscillation remains unclear. A fluctuation with a wavelength even smaller than $2Y^*$ cannot be rightly visualized as the type of undulatory motion, whether linear or nonlinear, executed bodily by the laminar flow. Rather, the short wavelength must be more representative of the turbulent motion, and the possibility remains that it is connected to the geometry of the turbulent front.

The spectral peak described in the previous paragraphs distorts the spectra to the point that the relation between transition and spectral evolution cannot be found at first glance. On the other hand, the possibility of a relation between the distorting peak and the evolution of the spectra cannot be discounted. Figure 9 shows an abrupt change in the high-frequency end of the spectrum in passing from $\bar{X} = -76$ to $\bar{X} = 76$. Beyond the latter the high-frequency content of the total fluctuation is substantial, although the logarithmic plot again tends to obscure the fact; also the energy content at frequencies below the peak frequency increases. In the transition zone therefore, the Fourier components on either side of the spectral peak become more active as the laminar oscillation becomes less active, as illustrated by Fig. 13. Furthermore Fig. 14 shows that the Fourier components adjacent to the peak increase the fastest, so that there is an apparent tendency of the peak oscillation to disperse its activity across the spectrum. Transition, therefore, seems to occur by spectral dispersion.§

§ The turbulence in the transition zone is intermittent, with the intermittency factor evolving from zero at the beginning of the zone to unity at its end.[25,26] This phenomenon, very interesting in itself, is an alternative description rather than an alternative explanation of the transition process.

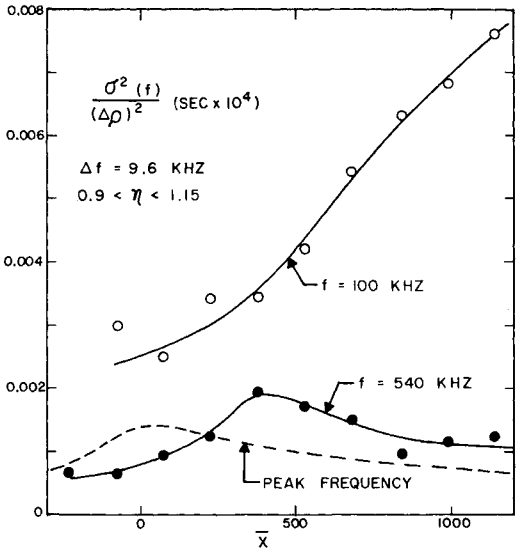

Fig. 13 Axial variation, along the maximum-shear region, of the spectral density of density fluctuations, for frequencies on either side of the peak frequency.

VIII. Concluding Discussion

If we accept, for the moment, that the observed oscillation in the laminar portion of the two-dimensional wake is a laminar instability responsible for the eventual breakdown into turbulence, we can synthesize the following picture from the quoted observations.

At some distance behind the body an originally weak oscillation appears with a wavelength about 4 times greater than the wake thickness $2Y^*$. By the time this oscillation has an intensity of about 10% of the local deficits it begins spreading to other Fourier components and distorting the mean velocity and temperature profiles. The point at which this distortion is first noted coincides with the virtual origin of the subsequently turbulent wake. In the next 500 wake thicknesses, the Prandtl number decreases slightly and the bulk kinematic viscosity increases greatly so that the wake slows and cools down. During this transition process, the fluctuation intensity continues increasing and its longitudinal integral scales decrease continuously. The end of transition is marked by the attainment of well-known self-preserving lateral profiles of velocity and temperature, the leveling off of the fluctuation intensities to a level characteristic of turbulent wakes and the decrease of the longitudinal scales to sizes representative of the turbulent microstructure.

It is important that at the end of transition the spectra of both the velocity and temperature are not rid of the peak remaining from the pretransitional activity. In the turbulent

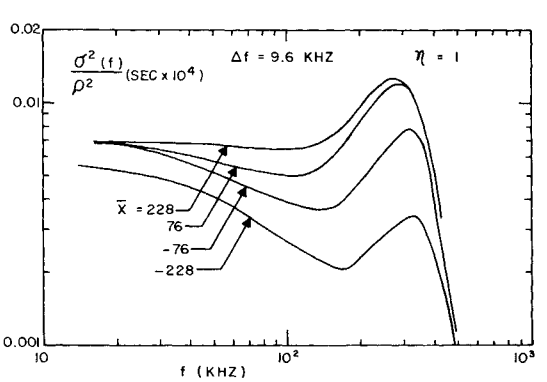

Fig. 14 Dispersion of the density fluctuation spectrum along the maximum-shear region.

wake this peak disperses much too slowly to be a mere remnant of the laminar oscillation. Furthermore in the transition zone the wavelength of this oscillation in relation to the wake thickness decreases by a factor of nearly three and ends up smaller than the wake thickness. The possibility thus arises that this is an interface (turbulent front) oscillation connected to turbulence instability, raising intriguing questions on which more research is needed.

In comparing these results with the earlier definitions of transition using the raw hot-wire output, of which Fig. 1 is an example, we find that the latter definitions put the transition point within the actual transition zone, as already anticipated by Gaviglio and Burnage.[26] The transition point lying at 800 C_Dh behind the body (see Fig. 1) translates to $\bar{X} = 300$ in the present experiment, whereas the actual transition zone extends from $\bar{X} = 0$ to 500. At first glance the raw-signal definition appears quite inaccurate. Nevertheless the transition zone is considerably contracted for axisymmetric wakes,[20] and even for two-dimensional geometries the 500 thicknesses C_Dh usually imply a smaller physical distance in terms of the body size. As a rough indicator of transition distance, the raw signal method is therefore acceptable, although proper diagnostics such as presented here are needed to define and understand the phenomenon more thoroughly.

References

[1] Demetriades, A. and Gold, H., "Transition to Turbulence in the Hypersonic Wakes of Blunt-Bluff Bodies," *ARS Journal*, Vol. 32, No. 4, Sept. 1963, p. 1420.

[2] Lees, L. and Gold, H., "Stability of Laminar Boundary Layer and Wakes at Hypersonic Speeds," *Proceedings of the International Symposium of Fundamental Phenomena in Hypersonic Flow*, Cornell University Press, 1966, p. 310.

[3] Liu, J. T. C., "Finite-Amplitude Instability of the Compressible Laminar Wake Weakly Non-Linear Theory," *The Physics of Fluids*, Vol. 12, No. 9, Sept. 1969, p. 1763.

[4] Ko, D. R., Kubota, T., and Lees, L., "Finite Disturbance Effect on the Stability of a Laminar Incompressible Wake Behind a Flat Plate," *Journal of Fluid Mechanics*, Vol. 40, Pt. 2, 1969, p. 315.

[5] Fay, J. A. and Goldburg, A., "Unsteady Hypersonic Wake Behind Blunt Bodies," *AIAA Journal*, Vol. 1, No. 10, Oct. 1963, p. 2264.

[6] Clay, W. G., Labitt, M., and Slattery, R. E., "Measured Transition from Laminar to Turbulent Flow and Subsequent Growth of Turbulent Wakes," *AIAA Journal*, Vol. 3, No. 5, May 1965, p. 837.

[7] Behrens, W., "Far Wake Behind Cylinders at Hypersonic Speeds: II Stability," *AIAA Journal*, Vol. 6, No. 2, Feb. 1968, p. 225.

[8] Batt, R. G., "Experimental Investigations of Wakes Behind Two-Dimensional Slender Bodies at Mach Number 6," Ph.D. thesis, California Inst. of Technology (GALCIT), Pasadena, Calif., June 1967.

[9] Demetriades, A., "Heat Transfer Effects on Supersonic Wake Transition," *The Physics of Fluids*, Vol. 13, No. 1, Jan 1970, p. 204.

[10] Behrens, W. and Ko, D., "Experimental Stability Studies in Wakes of Two-Dimensional Slender Bodies at Hypersonic Speeds," *AIAA Journal*, Vol. 9, No. 5, May 1971, pp. 851–857.

[11] Favre, A., Gaviglio, J., and Burnage, H., "Observations sur la Transition dans un Sillage en Ecoulement Supersonique," ONERA TP 499, 1967, Office Nationale d'Etudes et de Recherches Aeronautiques, Chatillon, France.

[12] Demetriades, A., "Turbulent Mean Flow Measurements in a Two-Dimensional Supersonic Wake," *The Physics of Fluids*, Vol. 12, No. 1, Jan. 1969, p. 24.

[13] Demetriades, A., "Turbulence Measurements in a Supersonic Two-Dimensional Wake," *The Physics of Fluids*, Vol. 13, No. 7, July 1970, p. 1672.

[14] Demetriades, A., "Hot-Wire Measurements in the Hypersonic Wakes of Slender Bodies," *AIAA Journal*, Vol. 2, No. 2, Feb. 1964, p. 245.

[15] Townsend, A. A., *The Structure of Turbulent Shear Flow*, Cambridge University Press, 1955, Chaps. 6, 7.

[16] Lees, L. and Hromas, L., "Turbulent Diffusion in the Wake of a Blunt Body at Hypersonic Speeds," *Journal of the Aeronautical Sciences*, Vol. 29, No. 8, Aug. 1962, p. 976.

[17] Gold, H., "Laminar Wake with Arbitrary Initial Profiles," *AIAA Journal*, Vol. 2, No. 5, May 1964, p. 948.

[18] Lin, C. C., ed., *Turbulent Flows and Heat Transfer*, Princeton University Press, Princeton, N. J., 1959, pp. 168–172.

[19] McCarthy, J. F., Jr. and Kubota, T., "A Study of Wakes Behind a Circular Cylinder at M = 5.7," *AIAA Journal*, Vol. 2, No. 4, April 1964, p. 629.

[20] Demetriades, A., "Turbulence Measurements in an Axisymmetric Compressible Wake," *The Physics of Fluids*, Vol. 11, No. 9, Sept. 1968, p. 1841.

[21] Demetriades, A., "Turbulence Front Structure of an Axisymmetric Compressible Wake," *Journal of Fluid Mechanics*, Vol. 34, Pt. 3, 1968, p. 465.

[22] Townsend, A. A., "The Mechanism of Entrainment in Free Turbulent Flows," *Journal of Fluid Mechanics*, Vol. 26, Pt. 4, 1966, p. 689.

[23] Grant, H. L., "The Large Eddies of Turbulent Motion," *Journal of Fluid Mechanics*, Vol. 4, 1958, p. 149.

[24] Sato, H. and Kuriki, K., "The Mechanism of Transition in the Wake of a Thin Flat Plate Placed Parallel to a Uniform Flow," *Journal of the Fluid Mechanics*, Vol. 11, Pt. 3, 1961, p. 321.

[25] Demetriades, A., "Observations on the Transition Process of Two-Dimensional Supersonic Wakes," AIAA Paper 70-793, Los Angeles, Calif., 1970.

[26] Gaviglio, J. and Burnage, H., "Sur L' Intermittance de Transition de L' etat Laminaire a L' etat Turbulent dans Divers Ecoulements," *Journal de Mecanique*, Vol. 9, No. 1, March 1970, p. 165.